

# Magnetization reversal of individual Fe nanowires in alumites studied by magnetic force microscopy

T. G. Sorop,<sup>a)</sup> C. Untiedt, F. Luis,<sup>b)</sup> and L. J. de Jongh  
*Kamerlingh Onnes Laboratory, Leiden University, 2300 RA Leiden, The Netherlands*

M. Kröll  
*Department of Physics, Trinity College Dublin, Dublin, Ireland*

M. Raşa  
*Van't Hoff Laboratory, Utrecht University, 3584 CH Utrecht, The Netherlands*

(Presented on 13 November 2002)

We have studied the magnetization reversal of two-dimensional (2D) arrays of parallel ferromagnetic Fe nanowires in nanoporous alumina templates. Combining bulk magnetization measurements using a superconducting quantum interference device with field-dependent magnetic force microscopy (MFM), we decomposed the macroscopic hysteresis loop in terms of irreversible magnetic responses of individual nanowires. The field-dependent MFM provides a microscopic method by which to obtain the hysteresis curve by registering the fraction of upward and downward magnetized wires for each field. The nanowire system proves to be an excellent example of the 2D classical Preisach model, well-known from the field of hysteresis modeling and micromagnetism. © 2003 American Institute of Physics. [DOI: 10.1063/1.1557397]

## I. INTRODUCTION

Periodic arrays of ferromagnetic nanoparticles or nanowires are currently attracting great interest due to their potential for numerous applications, as well as for providing a model system for the study of magnetic interactions and switching behavior. A procedure to fabricate arrays of metallic nanowires is to use as templates nanoporous materials, such as track-etched polymer membranes and anodized aluminum films, and fill the pores with metal by electrodeposition. A particular advantage of the alumina templates is that the nanopores are parallel, with the long axis perpendicular to the film surface, and have aspect ratios that can be as high as  $10^3$ . Recent work has addressed optimizing structural properties such as homogeneity of the pore size, pore distance, pore filling, and regularity of the superlattice.<sup>1</sup>

Our group has previously prepared Fe, Co, and Ni alumites and studied their magnetic properties.<sup>2</sup> The pore diameters  $D_p$  varied from 50 down to 6 nm, i.e., the same length scale and even smaller than the values of the domain wall widths  $\lambda_w$ . From the size dependence of the low temperature coercive field  $B_c$ , clear deviation from the curling mode prediction was found for  $D_p < \sqrt{\pi}\lambda_w$ , in good agreement with theoretical predictions<sup>3</sup> for nonuniform magnetization reversal by solitonic excitations near the ends of the wires.

The aim of the present work is to further investigate the reversal mechanism of these ferromagnetic nanowires, the role of the interwire dipolar interactions, and the way in which the responses of the individual wires combine and give the macroscopic hysteresis loop of the array. To achieve this, we have combined standard bulk magnetization mea-

surements [using superconducting quantum interference device (SQUID) magnetometry] with microscopic techniques such as atomic force microscopy (AFM) and field-dependent magnetic force microscopy (MFM).

## II. EXPERIMENTS AND DISCUSSION

Fe-filled alumite membranes were prepared and characterized by the method described in Ref. 2. The morphology and size of the pores were determined by scanning electron microscopy (SEM) and transmission electron microscopy (TEM), and by AFM. The pores proved to be uniform in size, well separated and formed a regular hexagonal structure. For this work, we chose samples with  $D_p = 50$  nm, where the hexagonal order is known to extend over large distances. For smaller sizes the thermal relaxation effects become important.<sup>2</sup> The AFM/MFM measurements were performed on the bottom face of the wire array after removal of the Al layer and the barrier layer. We only present data obtained for two representative samples (labeled Fe-1 and Fe-2), although similar results were obtained for other samples with different filling fractions and/or aspect ratios of the wires. Cross-sectional side-view TEM images show that each alumite membrane is divided into regions of pores completely filled from top to bottom, separated by regions of completely empty pores.

The magnetization was measured with a commercial SQUID magnetometer with the magnetic field parallel to the wires. A commercial NanoScope III (Digital Instruments) scanning probe microscope was used for the AFM/MFM measurements. Magnetic tips premagnetized to saturation, with radii of 40–60 nm and high coercivity ( $B_c \geq 0.5$  T), were used. The MFM images were recorded in dynamic mode at a scan height of about 30–50 nm. In order to perform MFM experiments in an external magnetic field, a

<sup>a)</sup>Electronic mail: sorop@phys.leidenuniv.nl

<sup>b)</sup>Permanent address: Instituto de Ciencia de Materiales de Aragón, CSIC–Universidad de Zaragoza, 50009 Zaragoza, Spain.

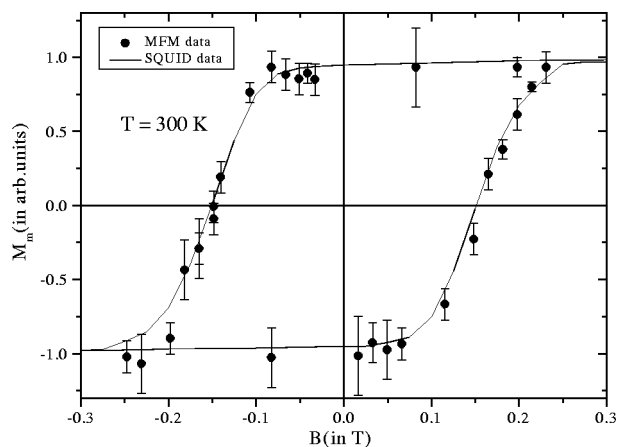


FIG. 1. Hysteresis loop of sample Fe-1 measured by SQUID magnetometry (solid line). The data points were obtained from the MFM images (cf. Fig. 2).

homemade coil (similar to that described in Ref. 4) was mounted onto the scanner. The coil generated field pulses up to 0.5 T, parallel to the wires and constant (less than 5% error) over 6 mm along this direction. Before each scan, a short pulse (rise time 160  $\mu$ s) corresponding to the target field value was first applied, with the magnetic tip retracted. After a few seconds, the magnetic tip was engaged and the AFM/MFM images were recorded.

Figure 1 shows the room temperature hysteresis loop for sample Fe-1 (solid curve) measured by SQUID magnetometry (field parallel to the wires). Note the high ratio of remanence to saturation (i.e., squareness)  $M_r/M_s \approx 0.97$ . Moreover, we found that  $M_r/M_s$  at room temperature does not deviate much from its value at 5 K, which shows that even at 300 K all wires remain in the initial state after the saturating magnetic field is removed. Since we wish to compare the macroscopic SQUID measurements with the results obtained with pulsed fields from the MFM images, we also measured the hysteresis loop of the remanent magnetization  $M_r(B)$  with the SQUID and obtained a  $M_r(B)$  curve very close to the magnetization loop measured in the usual way, which confirms that the magnetization changes mainly via irreversible processes.

By comparing the AFM/MFM images it could clearly be seen that the topography and the magnetic contrast are well separated. As the external field was varied, we saw no change in the topographic images only in the magnetic ones. We therefore restrict the discussion to the magnetic images. Figure 2 shows a series of images of the same region ( $3.5 \times 3.5 \mu\text{m}^2$ ) for different amplitudes of pulsed magnetic field. We first applied a pulsed field of 0.23 T parallel to the tip magnetization. Since this field exceeds the saturation field, the magnetic moments of all wires are aligned and appear with the same (bright) contrast in Fig. 2(a). The darker regions are associated with the empty pores. Next, a hysteresis-type cycle was performed with the pulsed field, following the same procedure as that for the SQUID measurement of  $M_r(B)$ . The MFM images taken in this same region do not show any noticeable change until a negative field of about  $-0.08$  T is applied [Fig. 2(b)], at which some

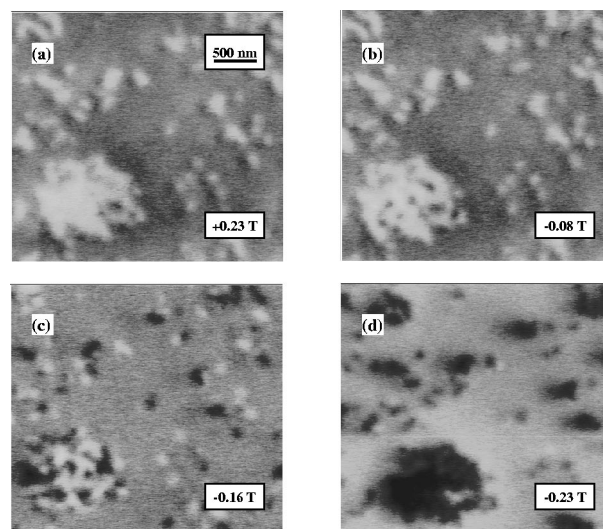


FIG. 2. Succession of MFM images of the same area ( $3.5 \times 3.5 \mu\text{m}^2$ ) of sample Fe-1 seen in Fig. 1, for field values of (a)  $B = 0.23$  T, and in the opposite direction and of  $B =$  (b)  $-0.08$ , (c)  $-0.16$ , and (d)  $-0.23$  T.

of the bright spots are seen to turn dark, indicating the reversal of magnetization for some of the wires. Further increases in the magnetic field cause the number of reversed wires to grow and in Fig. 2(c) one can observe that near the average coercive field ( $B_c = 0.15$  T) the number of reversed, and not-yet-reversed, wires has become roughly equal; thus the average magnetization on this microscopic scale is approximately zero, just as for the macroscopic curve. Finally, when  $B = -0.23$  T all wires are reversed [Fig. 2(d)]. This last image is the inverse of the first [Fig. 2(a)], and the empty regions now appear brightest. Images taken when performing the cycle from  $B = -0.23$  to  $+0.23$  T show the same changes in contrast but with opposite sign.

These results confirm that MFM images provide a means by which to construct the macroscopic magnetization curve by simply counting the number of wires with “upward” and “downward” directions for each field applied. Similar conclusions were recently reached by other groups.<sup>5–7</sup> The data obtained by this “microscopic technique” are compared to the SQUID hysteresis loop in Fig. 1 and show very good agreement in shape, symmetry, and the values of coercive and saturation fields. We can conclude that the macroscopic hysteresis loop is actually composed of contributions by irreversibly switching individual nanowires. For high-aspect ratio wires such as ours, this result is certainly nontrivial since the AFM/MFM is only sensitive to the ends of the wires, whereas the SQUID measures the volume magnetization. Thus, the apparent agreement between the two measurements proves that the Fe nanowires are indeed *monodomain* ferromagnetic needles.

In principle the observed distribution of the individual switching fields  $B_c$ , which causes rounding of the macroscopic hysteresis loop, can be related either to differences in morphology of the wires or to interwire dipolar interactions. However the TEM images for our samples show a regular structure, with very long straight wires and only a small distribution of diameters and length. Therefore, the dominant

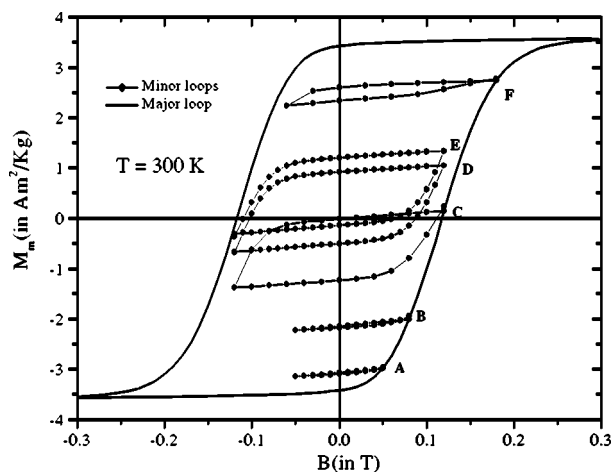


FIG. 3. SQUID data for sample Fe-2, illustrating the properties of wiping out (loops A, B, C, and F) and congruency (loops C, D, and E).

source of the broadening is most probably a distribution in the dipolar field caused by dipole–dipole interaction between the wires. In view of the inhomogeneous filling of the pores in the templates, a large spatial variation in the dipolar field felt by the wires is indeed to be expected. The effects of the interwire dipolar interactions were studied by measuring the switching behavior of single wire, in different regions of the samples, from which it became quite clear that the hysteresis loops of individual wires are highly asymmetric (displaced along the applied field axis with respect to the origin) with large variation in displacement and large variation in the degree of asymmetry. From these experiments we conclude that interwire dipolar interactions can reach values as high as 0.15 T when expressed in terms of an effective field. This value can be compared with the dipolar coupling estimated following the model in Ref. 8. We calculated the difference in switching field for an isolated element and an element immersed in an array of successive shells of parallel neighbors in a hexagonal array. Including contributions from the first 20 neighboring shells the model yields a value for  $\Delta B_s$  of about 0.13 T. The dipolar coupling *between* filled regions is found to be quite small ( $\approx 1$  mT), so they can safely be neglected. It is also clear from the model that a wire at the periphery of a filled region will experience a dipolar field quite different from one in the center.

We end by noting that the nanowire system turns out to be an excellent example of the well-known classical Preisach model for hysteresis.<sup>9,10</sup> In this model, the statistics of the hysteresis loops of individual single-domain particles determines the shape of the macroscopic major and minor loops.

According to Mayergoyz<sup>11</sup> the “congruency” and the “wiping out” properties of the minor loops are necessary and sufficient conditions for a hysteretic system to be described by a classical Preisach model. In order to check this, appropriate sets of magnetization data were measured for sample Fe-2 with the SQUID. In Fig. 3 the minor loops starting at A, B, C, and F close at their initial value of magnetization. This means that the variations in field have erased (wiped out) past history, i.e., the system has a wiping out property. Also in Fig. 3 minor loops C, D, and E with the same limiting field of  $\pm 0.12$  T are shown. All these minor loops have the same shape and the same enclosed area, i.e., they are geometrically congruent and the system exhibits the property of congruency. We conclude that, even for highly diluted (low filling fraction) two-dimensional arrays such as those studied here, the requirements for the Preisach model are apparently met. Perhaps surprising at first is the intrinsic distribution in the interaction that arises from incomplete filling does not render the model invalid.

## ACKNOWLEDGMENTS

This work was part of the research program of the Stichting voor Fundamenteel Onderzoek der Materie (FOM). Two of the authors (C.U. and F.L.) acknowledge grants from the European Union under the TMR Program. Two other authors acknowledge a grant by the Deutsche Forschungsgemeinschaft (M.K.) and the Colloid Physics Stimulation Program of Utrecht University (M.R.). The authors thank A. P. Philippe and A. Morello for their interest and help with the experiments.

- <sup>1</sup>A. P. Li, F. Müller, A. Birner, K. Nielsch, and U. Gösele, *J. Appl. Phys.* **84**, 6023 (1998); A. J. Yin, J. Li, W. Jian, A. J. Bennett, and J. M. Xu, *Appl. Phys. Lett.* **79**, 1039 (2001); K. Nielsch, F. Müller, A. P. Li, and U. Gösele, *Adv. Mater.* **12**, 582 (2000).
- <sup>2</sup>P. M. Paulus, F. Luis, M. Kröll, G. Schmid, and L. J. de Jongh, *J. Magn. Magn. Mater.* **224**, 180 (2001).
- <sup>3</sup>H.-B. Braun, *Phys. Rev. Lett.* **71**, 3557 (1993); *J. Appl. Phys.* **85**, 6172 (1999).
- <sup>4</sup>S. Manalis, K. Babcock, J. Massie, V. Elings, and M. Douglas, *Appl. Phys. Lett.* **66**, 2585 (1995).
- <sup>5</sup>C. A. Ross *et al.*, *Phys. Rev. B* **65**, 144417 (2002).
- <sup>6</sup>G. A. Gibson and S. Schultz, *J. Appl. Phys.* **73**, 4516 (1993).
- <sup>7</sup>K. Nielsch, R. B. Wehrspohn, J. Barthel, J. Kirschner, U. Gösele, S. F. Fischer, and H. Kronmüller, *Appl. Phys. Lett.* **79**, 1360 (2001); K. Nielsch, R. B. Wehrspohn, J. Barthel, J. Kirschner, S. F. Fischer, T. Schweinböck, D. Weiss, and U. Gösele, *J. Magn. Magn. Mater.* **249**, 234 (2002).
- <sup>8</sup>Y. Ishii and M. Sato, *J. Magn. Magn. Mater.* **82**, 309 (1989); E. O. Samwell, P. R. Bissell, and J. C. Lodder, *ibid.* **115**, 327 (1992).
- <sup>9</sup>F. Preisach, *Z. Phys.* **94**, 277 (1935).
- <sup>10</sup>M. Pardavi-Horvath, G. Zheng, and G. Vertesy, *Physica B* **233**, 287 (1997).
- <sup>11</sup>I. D. Mayergoyz, *Phys. Rev. Lett.* **56**, 1518 (1986).